Wojciech RYNIEWICZ[*]**, Łukasz BOJKO**[**]**, Anna M. RYNIEWICZ**[***]**,
Małgorzata PIHUT**[****]**, Paweł PAŁKA**[*****]

TRIBOLOGICAL STUDIES OF LAYERED BIOMATERIALS FOR PROSTHETIC STRUCTURES BASED ON SUBSTRUCTURES MADE OF DIGITAL TECHNOLOGIES

BADANIA TRIBOLOGICZNE BIOMATERIAŁÓW WARSTWOWYCH NA KONSTRUKCJE PROTETYCZNE O PODBUDOWACH Z TECHNOLOGII CYFROWYCH

Key words:	digital technologies, prosthetic substructures, veneering ceramics, friction, wear, SEM.
Abstract	Modern dental prosthetics uses CAD/CAM in the Computer Aided Design (CAD) of substructures and its Computer Aided Manufacturing (CAM) process. The substructure is subject to appropriate veneering, which determines the functional cooperation. The aim of this study is to investigate the friction coefficient and wear resistance of the veneering layers of the substructures of prosthetic structures. The test materials are dedicated veneering layers on substructures made of factory-made CoCr, TiCP, and Ti6Al4V metal fittings as well as the glass-ceramic material $LiSi_2$ and the ceramic ZrO_2. The study was conducted on a Roxana Machine Works tribological machine in the ball-and-3discs system in an artificial saliva environment using a Hitachi S3400 scanning microscope. As a reference biomaterial, enamel-dentin discs were used. The tribological processes that take place under chewing conditions in the presence of saliva depend on the properties and technological parameters of the surface layer of the biomaterial wearing out and on the enamel of opposing teeth in contact, which also wears out. They should reproduce the physiological nature of adjustment wear in the stomatognathic system (SS). The determined values of the friction coefficient and wear resistance allowed differences to be indicated in the course of tribological processes, and microscopic analyses confirmed them.
Słowa kluczowe:	technologie cyfrowe, podbudowy protetyczne, ceramiki licujące, tarcie, zużycie, SEM.
Streszczenie	Współczesna protetyka stomatologiczna wykorzystuje system CAD/CAM do cyfrowego projektowania podbudowy konstrukcji (CAD) oraz do jej wytwarzania w sterowanym numerycznie procesie (CAM). Podbudowa nośna poddawana jest odpowiedniemu licowaniu, które decyduje o funkcjonalnej współpracy. Celem pracy jest badanie współczynnika tarcia i odporności na zużycie warstw licujących podbudowy konstrukcji protetycznych. Materiałem badań są dedykowane warstwy licujące na podbudowach wykonanych w technologii frezowania z fabrycznych kształtek z metali – CoCr, TiCP i Ti6Al4V oraz z materiałów szklano-ceramicznych $LiSi_2$ i ceramicznych ZrO_2. Badania wykonano na maszynie tribologicznej Roxana Machine Works w układzie kula-3krążki w środowisku sztucznej śliny oraz na mikroskopie skaningowym Hitachi S3400. Jako biomateriał referencyjny wykorzystano krążki szkliwno-zębinowe. Procesy tribologiczne, które zachodzą w warunkach żucia w obecności śliny uzależnione są od właściwości i parametrów technologicznych warstwy wierzchniej zużywającego się biomateriału oraz od szkliwa zębów przeciwstawnych wchodzących w kontakt, które również się zużywają. Powinny odtwarzać fizjologiczny charakter zużycia dostosowawczego w układzie stomatognatycznym (US). Wyznaczone wartości współczynnika tarcia i odporności na zużycie pozwoliły na wskazanie różnic w przebiegu procesów tribologicznych, a analizy mikroskopowe to potwierdziły.

[*]   ORCID: 0000-0002-9140-198X. Jagiellonian University Medical College, Faculty of Medicine, Dental Institute, Department of Dental Prosthodontics, Montelupich 4 Street, 31-155 Cracow, Poland.

[**]   ORCID: 0000-0002-6024-458X. AGH University of Science and Technology, Faculty of Mechanical Engineering and Robotics, Mickiewicza 30 Ave., 30-059 Cracow, Poland.

[***]   ORCID: 0000-0003-2469-6527. Jagiellonian University Medical College, Faculty of Medicine, Dental Institute, Department of Dental Prosthodontics, Montelupich 4 Street, 31-155 Cracow, Poland.

[****]   ORCID: 0000-0003-2670-966X. Jagiellonian University Medical College, Faculty of Medicine, Dental Institute, Department of Dental Prosthodontics, Montelupich 4 Street, 31-155 Cracow, Poland.

[*****] ORCID: 0000-0003-0640-7939. AGH University of Science and Technology, Faculty of Non-Ferrous Metals, Mickiewicza 30 Ave., 30-059 Cracow, Poland.

INTRODUCTION

Prosthetic crowns reproduce the damaged hard structures of the patient's own teeth and take over their natural functions [L. 1–6]. They may constitute independent fillings or are components of multiple tooth permanent dentures and/or serve as an anchorage of partial removable dentures. The most important functions of the prosthetic structures include the following: effective participation in the act of chewing and speaking, maintaining the continuity of dental arches and the occlusal surface, the protection of periodontal tissues, and providing physiological conditions for occlusal load transfer [L. 7]. They are layered structures and the substructure can be made of metals, alloys, glass ceramic, and ceramic materials. The supporting structure of the crown or bridge, depending on the biomaterial used and the manufacturing technology, is subject to veneering [L. 4, 8–10]. Ceramic veneering layers of the substructures are responsible for functional and tribological cooperation with opposing teeth. One of the most important criteria for the assessment of veneering layers is their tribological parameters in contact with chewing surfaces. In order to ensure the proper functioning of the SS, it is necessary to restore missing tissues in a way that is as close as possible to natural dentition in terms of biomechanics, biotribology, and aesthetics [L. 6, 11, 12]. The undertaken study has been carried out in cooperation with the Department of Prosthetic Dentistry of the Jagiellonian University Medical College and the Department of Machine Construction and Operation of the AGH University of Science and Technology.

The aim of the study is to evaluate ceramic layers veneering prosthetic structures produced in the technology of milling from factory blocks and in the technology of laser sintering from metal powders, in terms of the following:

- Determining the coefficient of friction and wear resistance in the environment of artificial saliva (0.4 g NaCl; 0.4 g KCl; 0.795 g $CaCl_2$ x $2H_2O$; 0.78 g NaH_2PO_4 x $2H_2O$; 0.005 g Na_2S x 9 H_2O; 1g of urea for 1 litre of distilled water), in sliding friction conditions during loaded concentrated contact; and,
- Microscopic analysis of the surface layer structure after the veneering process and after the wear process.

MATERIAL AND METHOD

The study material includes ceramic veneering layers dedicated to metal, glass-ceramic, and ceramic substructures manufactured using digital technologies. The test specimen kits have been prepared in professional laboratories in accordance with the latest knowledge on innovative prosthetic construction technologies.

Samples made of materials for supporting substructures in the form of discs ø1/4", 1/16" thick, in sets of 30 pieces each, were made in the CAD/CAM system using two technologies. A CORiTEC 350i-imes-icore device was used to produce discs in the milling technology with factory fittings made of the following biomaterials: CoCrMo alloy, TiCP titanium, Ti6Al4V alloy, $LiSi_2$ ceramics, and ZrO_2 ceramics. ZrO_2 ceramic discs were milled correspondingly larger and were then subjected to a sintering process to achieve the proper structure and dimensions required for testing. Discs made of materials for supporting substructures using the Selective Laser Melting (SLM) technology were sintered with selective metal powders in a Renishaw AM250 device. Substrate samples from CoCrMo and Ti6Al4V were prepared using the incremental method. The discs prepared in this way and produced using both digital technologies were subjected to the processes of veneering with dedicated ceramics in the Dental Ceramics Laboratory. The veneering was carried out in the application of appropriate ceramic layers and their firing in the processes recommended for the applied system [L. 3, 13]. The test samples were veneered with the following systems: Duceram Kiss set of the CoCrMo substructure from milling, Duceram Kiss set of a substructure with SLM, ultra-low-melting Vita Titankeramik ceramic of the TiCP substructure from milling, ultra-low-melting Vita Titankeramik ceramic of the Ti6Al4V substructure from milling, ultra-low-melting Vita Titankeramik ceramic of the Ti6Al4V substructure from SLM, nanofluoroapatite glass ceramic IPS e.max Ceram of the $LiSi_2$ substructure from milling, and Elephant Sakura silicone ceramic of the ZrO_2 substructure from milling and sintering. Enamel specimens obtained in the form of discs from normal premolars and molars were used as reference materials and removed for periodontologic reasons. Samples were kept for 48 hours in a saline solution.

The tests of the coefficient of friction and wear resistance in sliding contact were conducted in the presence of artificial saliva. Saliva is a medium with a high content of enzymes and plays an extremely important role in the lubrication of cooperating occlusion surfaces [L. 14]. Tribological tests were carried out on a Roxana Machine Works apparatus, using a friction pair consisting of a ball and three discs from the tested material (Fig. 1). The counter-specimens were standard ceramic balls (Sø 1/2") made of zirconium oxide, with a deviation of 0.00013mm according to ASTM F2094-02a. The microstructure of the surface layer before the wear process and in the wear defect zone was recorded using a Hitachi S-3400N scanning microscope after prior carbon deposition.

The geometry of the research node approximated the spatial system found in the SS [L. 15]. It allowed us to imitate the change in wear intensity observed during *in vivo* studies, which is associated with a change in the
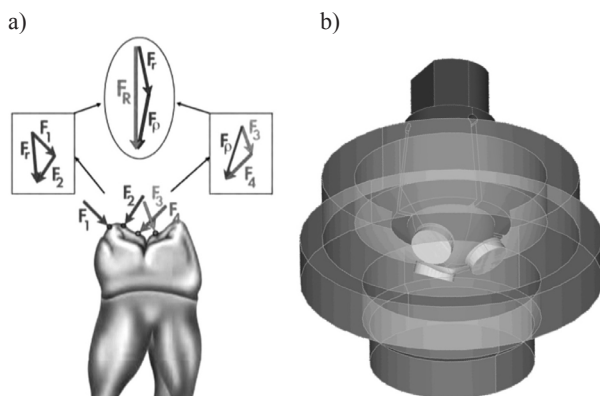
a)   b)

Fig. 1. **Spatial system of forces in occlusal contact in the SS (a), friction node geometry in a ball–and–3discs system (b) [L. 15]**

Rys. 1. Przestrzenny układ sił w kontaktach okluzyjnych (a), geometria węzła tarcia w układzie kula – 3 krążki (b) [L. 15]

contact surface area. The tests were performed with the following parameters:
– Rotational speed = 200 RPM ±5 RPM,
– Operation temperature = 36.6°C ±1°C;
– Load = 100 N ±3N,
– Duration = 15 min ±5 s.

The average wear defect diameter was a measure of the anti-wear properties of the tested materials. During the tests, continuous friction torque was recorded and, on this basis, the coefficient of friction was determined.

The results were statistically analysed using the Statistica 13.1 software (StatSoft).

The following were determined:
1) Descriptive statistics (average, median, min, max, std. deviation),
2) Normality of variable distribution (Shapiro-Wilk, Kolmogorov-Smirnov test),
3) Analysis of variance tests (ANOVA), and
4) Test of multiple post-hoc comparisons (Tukey, Bonferroni).

The statistical significance level was assumed as $p = 0.05$.

RESULTS

Under steady state conditions, there are no significant differences in the test results of the friction coefficients of the assessed veneering layers **(Figs. 2–5)**. The coefficients of friction are within the 0.55–0.75 range. They are slightly higher than the enamel coefficient of friction, which, under steady state conditions, is 0.50 on average. The difference in the friction coefficient of veneering layers and enamel in the initial course is characteristic. The coefficient of friction of the enamel develops slowly from 0.20 to 0.50 and stabilizes, while the coefficients of friction of the test samples in the initial phase of the test run are much higher, with a higher amplitude than under steady state conditions. The friction coefficients of the veneered layers in the Duceram Kiss system on the CoCrMo milling substructures are 0.68 and higher than the same veneering layers on the CoCrMo SLM technology substructures for which they are 0.60 **(Fig. 2)**. Differences in the values of friction coefficients are greater in the initial conditions in the same order.
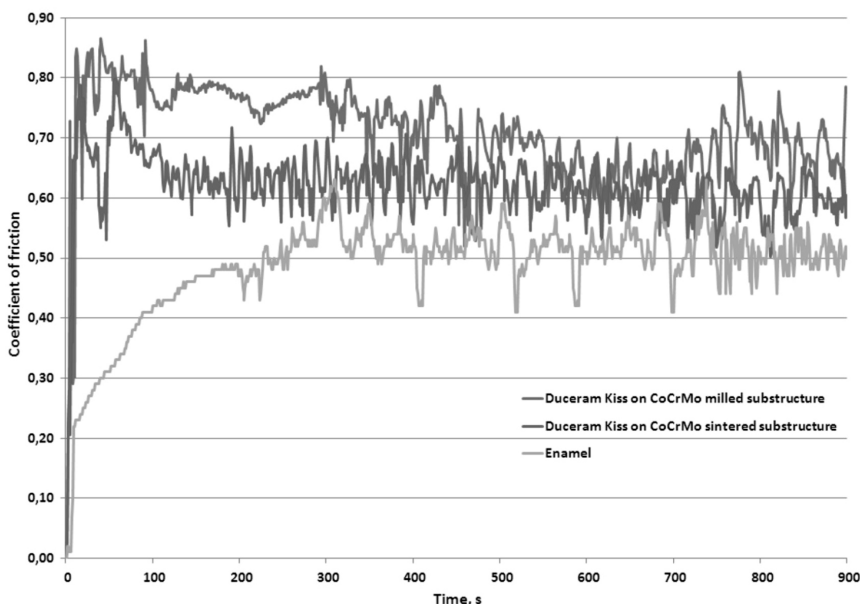

Fig. 2. **Friction coefficients of the Duceram Kiss veneering layers on CoCrMo milling and SLM technology substructures compared to enamel**

Rys. 2. Współczynniki tarcia warstw licujących Duceram Kiss na podbudowach CoCrMo z technologii frezowania oraz z technologii SLM, w porównaniu ze szkliwem
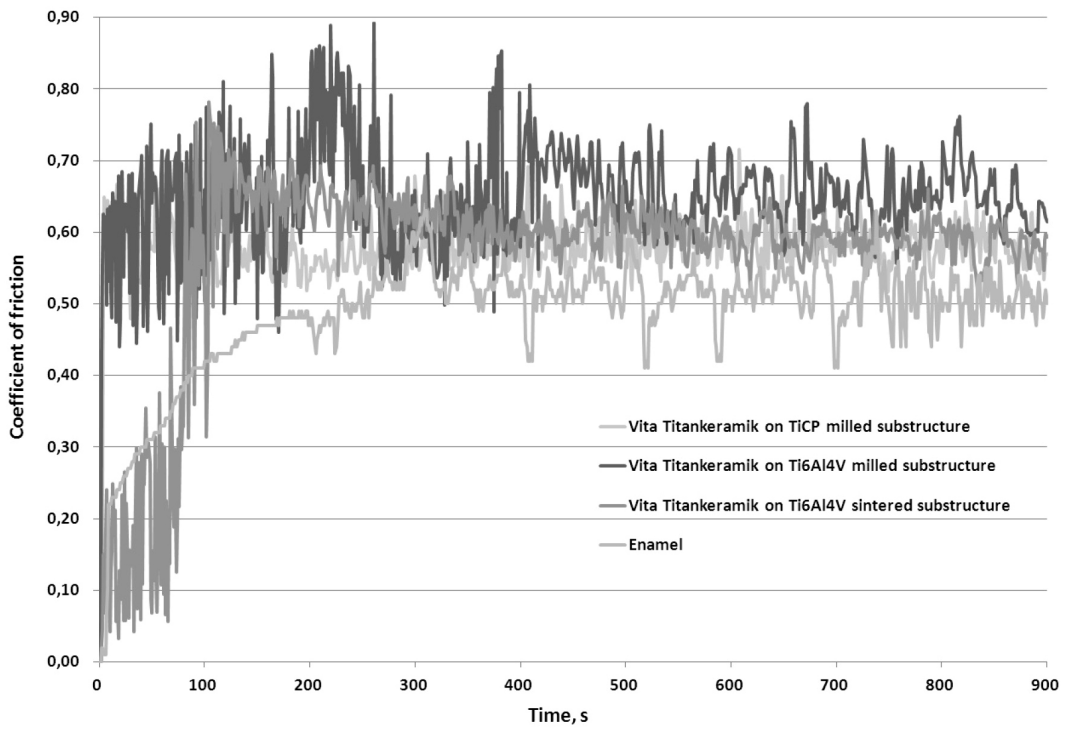
Fig. 3. **Friction coefficients of the Vita Titankeramik veneering layers on a pure titanium milled substructure, and the Ti6Al4V substructures from milling and SLM technology compared to enamel**

Rys. 3. Współczynniki tarcia warstw licujących Vita Titankeramik na podbudowie frezowanej z czystego tytanu oraz na podbudowach Ti6Al4V z technologii frezowania oraz z technologii SLM, w porównaniu ze szkliwem
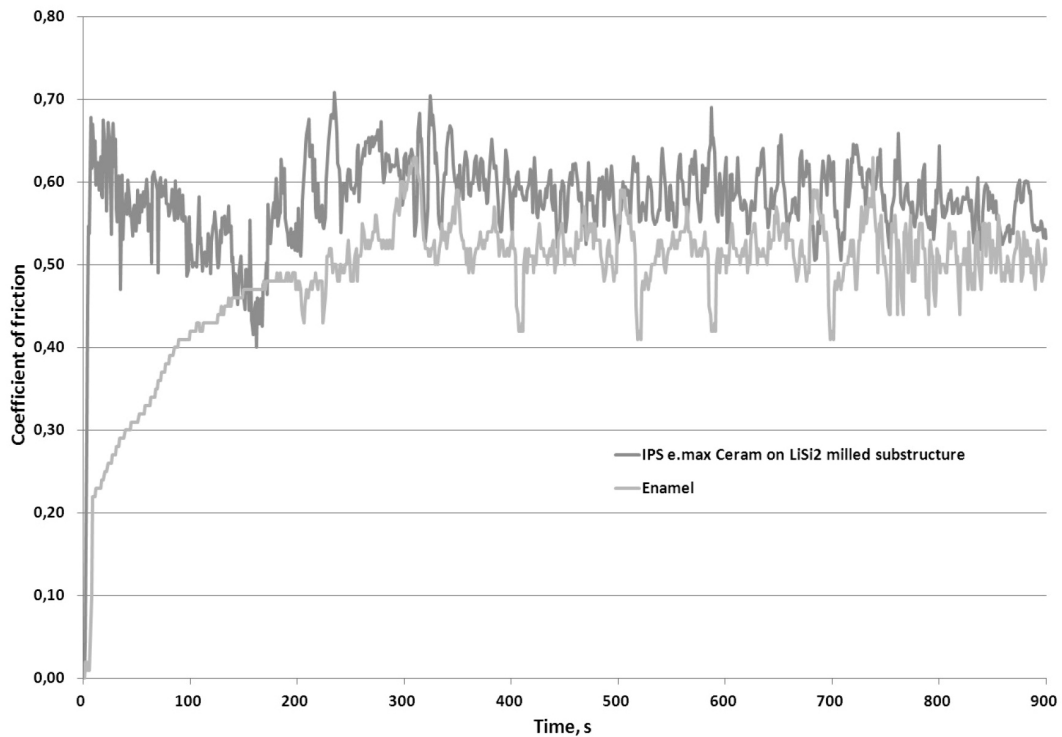

Fig. 4. **Friction coefficients of the IPS e.max Ceram veneering layer on the LiSi$_2$ substructure with milling technology, compared to enamel**

Rys. 4. Współczynniki tarcia warstwy licującej IPS e.max Ceram na podbudowie LiSi$_2$ z technologii frezowania, w porównaniu ze szkliwem
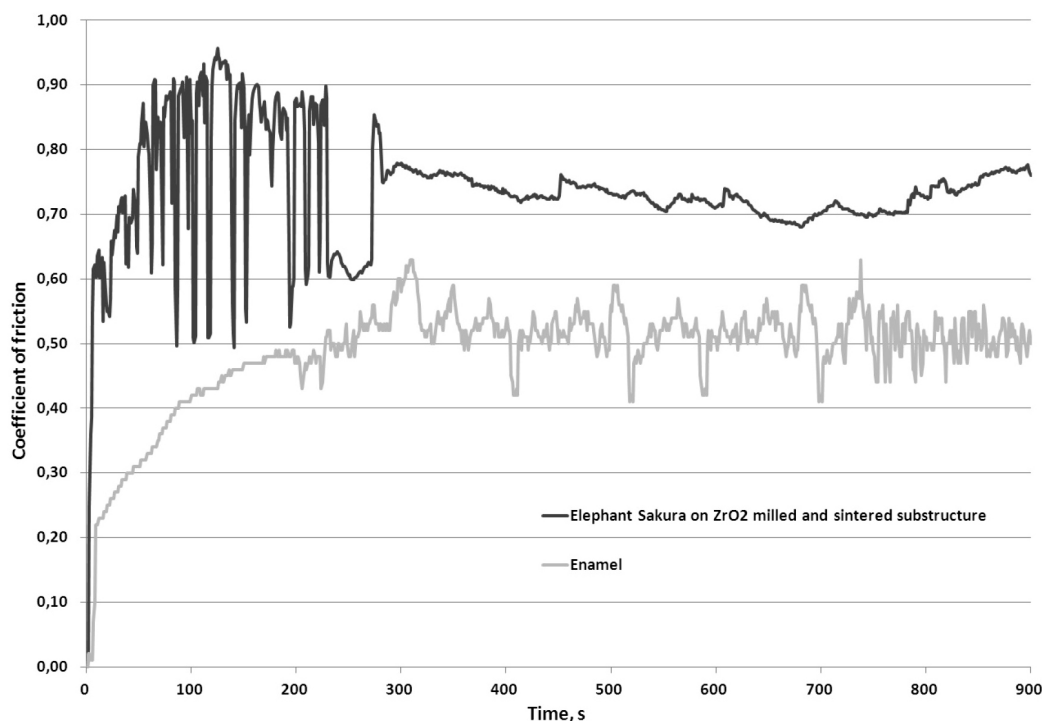
Fig. 5. Friction coefficients of the Elephant Sakura veneering layer on the ZrO$_2$ substructure with milling and synthetizing technology compared to enamel

Rys. 5. Współczynniki tarcia warstwy licującej Elephant Sakura na podbudowie ZrO$_2$ z technologii frezowania i syntetyzacji, w porównaniu ze szkliwem

The coefficient of friction of the veneered layers for ultra-low-melting Vita Titankeramik ceramics on the Ti6Al4V milling substructures is 0.65 on average. It is higher than the friction coefficient on the TiCP milling substructures, which is 0.60, and the friction coefficient on Ti6Al4V using SLM technology, which is also 0.60 **(Fig. 3)**. The courses of friction coefficients on titanium using Vita Titankeramik ceramics, in the initial conditions, have unstable and strongly increasing courses compared to the values indicated above.

The coefficient of friction of layers veneered with the nanofluoroapatite glass ceramics IPS e.max Ceram of the LiSi$_2$ milling substructure in steady state conditions is 0.58 on average, and it has values slightly higher than those of enamel, for which the coefficient of friction is 0.50 **(Fig. 4)**. In the initial course, the coefficient of friction in the IPS e.max Ceram veneering is at the level of the coefficient of friction under steady conditions, while in the enamel it rises slowly. The coefficient of friction of the layers veneered with Elephant Sakura silica ceramics of the ZrO$_2$ base from milling and sintering under steady conditions reaches a much higher value (0.72) than that of enamel **(Fig. 5)**. In the initial phase, the coefficient of friction is unstable with high amplitudes, and under steady state conditions, it is the mildest of all the tested layered materials.

The values of average diameters of wear defects allow the process of wear to be evaluated for different veneering layers on different substructures obtained from different technologies **(Fig. 6, Tab. 1)**. The highest wear values were found for veneering with the Duceram Kiss system on the CoCrMo substructure with SLM and the IPS e.max Ceram layer on the LiSi$_2$ substructure. The lowest values of wear defects from all the tested sets were observed for the Elephant Sakura veneering system on the ZrO$_2$ milling and sintering substructure. The veneering test with Duceram Kiss ceramics of CoCrMo substructures showed higher values of wear defects for SLM technology than for milling technology. In the case of Vita Titankeramik veneering of titanium substructures, the highest values of wear defects were observed for Ti6Al4V with SLM technology. They were slightly lower for Ti6Al4V with milling technology and the lowest for TiCP with milling technology. The wear resistance of the tested materials was characterized by parameters of descriptive statistics: mean value, standard deviation, and result distribution **(Fig. 6**, **Table 1)**. An example analysis of distribution normality is also presented for the Elephant Sakura veneering ceramics material on the ZrO$_2$ substructure **(Fig. 7)**, indicating a normal distribution. An insignificant difference between the diameters of the defects was obtained between the following materials: Duceram Kiss on the CoCrMo substructure with SLM technology and IPS e.max Ceram on the LiSi$_2$ base with milling. All other differences in mean defect diameters show statistical significance **(Tab. 2)**.
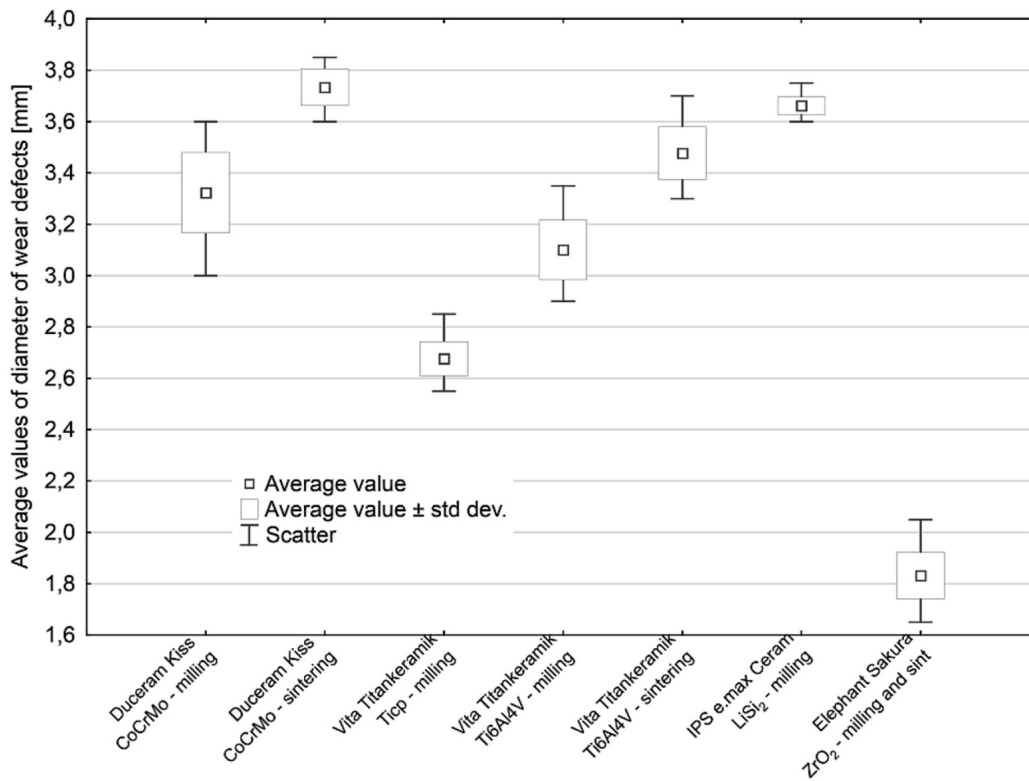
Fig. 6. Tests of wear resistance of veneering materials
Rys. 6. Badania odporności na zużycie materiałów licujących

Table 1. Statistical parameters of wear defects in the tested materials
Tabela 1. Parametry statystyczne skazy zużyciowej w badanych materiałach

Tested material		Statistical parameters for description				
The veneering layer	Substructure	Number of samples	Average value	Minimum value	Maximum value	Standard deviation
Duceram Kiss	**CoCrMo – milling**	30	3.32	3.00	3.60	0.154
	CoCrMo – sintering		3.73	3.60	3.85	0.071
Vita Titankeramik	**TiCP – milling**		2.68	2.55	2.85	0.066
	Ti6Al4V – milling		3.10	2.90	3.35	0.114
	Ti6Al4V – sintering		3.48	3.30	3.70	0.100
IPS e.max Ceram	**LiSi$_2$ – milling**		3.66	3.60	3.75	0.033
Elephant Sakura	**ZrO$_2$ – milling and sintering**		1.83	1.65	2.05	0.089

One may notice that, in the initial course, i.e. when the process runs from point contact to defect formation, in layered biomaterials for prosthetic structures, the processes of surface layer destruction differ from the processes of enamel destruction. The targeted structure of enamel prisms, their strength parameters, and compatibility with saliva affect the low friction coefficient, compared to the friction in materials for prosthetic structures. The courses and values of friction coefficients very close to each other do not translate into wear resistance of the tested materials. When analysing the results for metal substructures, it can be seen that the same veneering layer has lower defect values, and lower hardness of the substructure and Young's module [L. 9].

Summary: ZrO$_2$

Fig. 7. Example of normality distribution analysis for the Elephant Sakura veneering ceramics material on the ZrO$_2$ substructure

Rys. 7. Przykładowa analiza normalności rozkładu dla materiału ceramiki licującej Elephant Sakura na podbudowie ZrO$_2$

Table. 2. Statistical analysis results of diameters of wear defects in the *post hoc* ANOVA test (Bonferroni)

Tabela 2. Wyniki analiz statystycznych średnic skaz zużyciowych w teście ANOVA post hoc (Bonferroniego)

Bonferroni's test
Approximate probabilities for post hoc tests
Error: MS intergroup = 0.00963, df = 203.00

Material	Duceram Kiss on CoCrMo milled substructure	Duceram Kiss on CoCrMo sintered substructure	Vita Titankeramik on TiCP milled substructure	Vita Titankeramik on Ti6Al4V milled substructure	Vita Titankeramik on Ti6Al4V sintered substructure	IPS e.max. Ceram on LiSi$_2$ milled substructure	Elephant Sakura on ZrO$_2$ milled and sintered substructure
Duceram Kiss on CoCrMo milled substructure		0.00	0.00	0.00	0.00	0.00	0.00
Duceram Kiss on CoCrMo sintered substructure	0.00		0.00	0.00	0.00	0.109813	0.00
Vita Titankeramik on TiCP milled substructure	0.00	0.00		0.00	0.00	0.00	0.00
Vita Titankeramik on Ti6Al4V milled substructure	0.00	0.00	0.00		0.00	0.00	0.00
Vita Titankeramik on Ti6Al4V sintered substructure	0.00	0.00	0.00	0.00		0.00	0.00
IPS e.max. Ceram on LiSi$_2$ milled substructure	0.00	0.109813	0.00	0.00	0.00		0.00
Elephant Sakura on ZrO$_2$ milled and sintered substructure	0.00	0.00	0.00	0.00	0.00	0.00	

SEM images of surfaces veneered with Duceram Kiss ceramics on the CoCrMo substructures, after the process of firing the veneering layers, have a uniform structure with few porosities and slight unevenness and characteristic lines created during solidification (**Fig. 8a** and **Fig. 9a**). A defect on a milled substructure has a more regular edge than a defect on an SLM substructure (**Fig. 8b** and **Fig. 9b**). Images of wear defects show irregular wear and grain structure, which is especially visible in the veneering of the CoCrMo substructure with SLM technology (**Fig. 8c** and **Fig. 9c**).
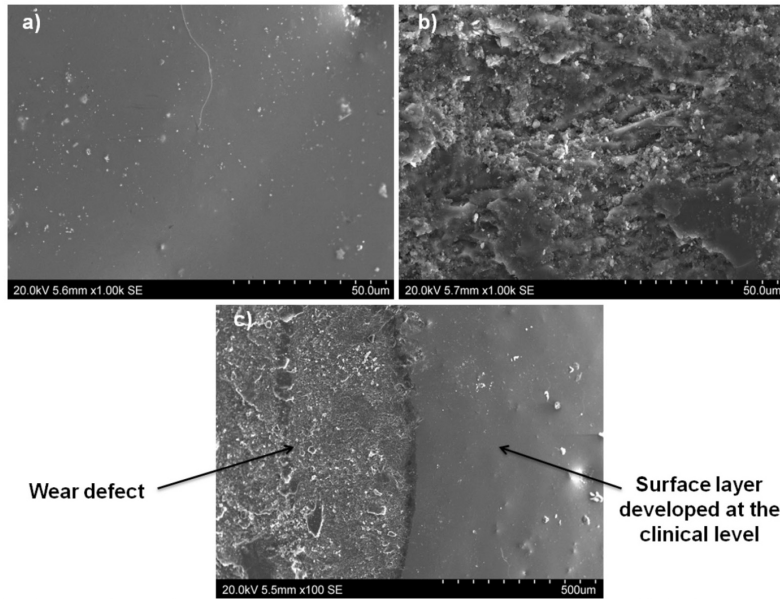
Fig. 8. **SEM images of the surface veneered with Duceram Kiss ceramics on the CoCrMo milled substructure: a) surface layer developed at the clinical level, b) surface layer in the defect after the wear test, c) boundary zone between the defect and the area before the wear test**

Rys. 8. Obrazy SEM powierzchni licowanej ceramiką Duceram Kiss na podbudowie CoCrMo frezowanej: a) warstwa wierzchnia opracowana na poziomie klinicznym, b) warstwa wierzchnia w skazie po badaniu zużyciowym, c) strefa granicy między skazą a obszarem przed badaniem zużyciowym
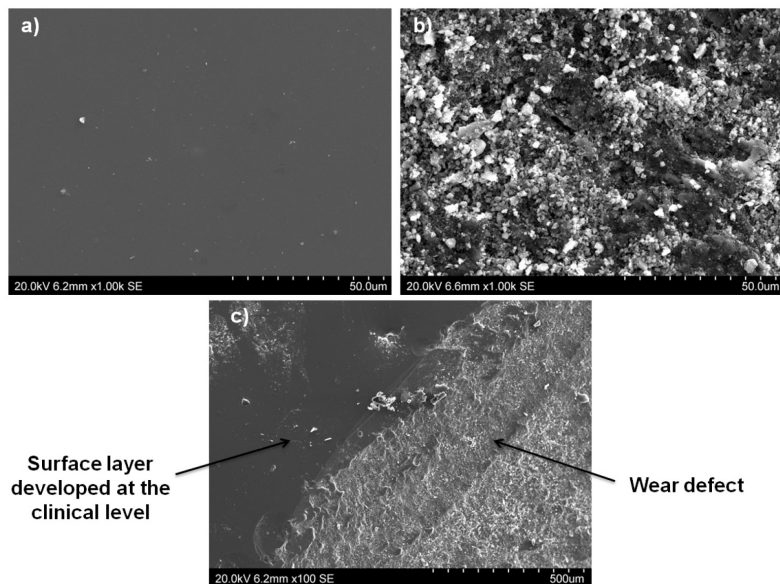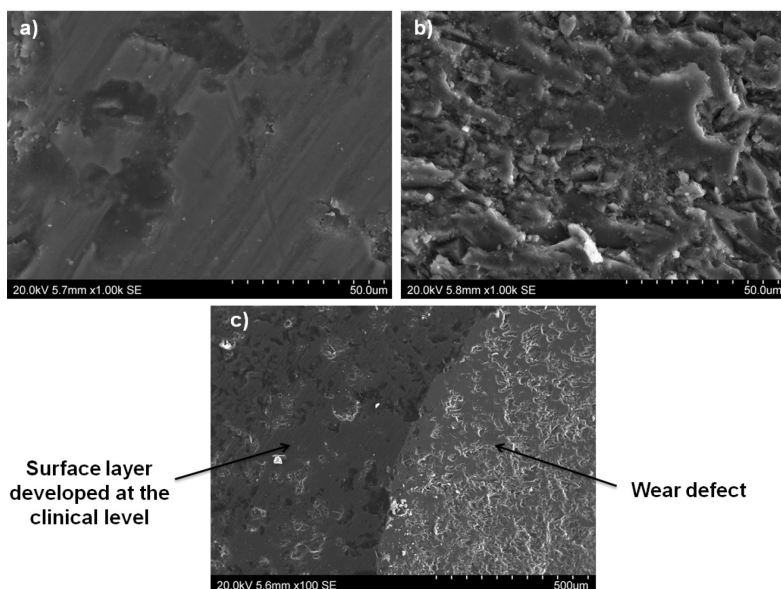
Fig. 9. **SEM images of the surface veneering Duceram Kiss ceramics on the CoCrMo incremental sintering substructure: a) surface layer developed at the clinical level, b) surface layer in the defect after the wear test, c) border zone between the defect and the area before the wear test**

Rys. 9. Obrazy SEM powierzchni licowanej ceramiką Duceram Kiss na podbudowie CoCrMo z przyrostowego spiekania: a) warstwa wierzchnia opracowana na poziomie klinicznym, b) warstwa wierzchnia w skazie po badaniu zużyciowym, c) strefa granicy między skazą a obszarem przed badaniem zużyciowym

SEM images of titanium substructures veneered with Vita Titankeramik ceramics show uneven structures after the veneering process **(Fig. 10a, Fig. 11a, Fig. 12a)**. In TiCP and Ti6Al4V veneering from milling, it is possible to see scratches, a few pores, and protrusions **(Fig. 10a, Fig. 11a)**. The largest pores and protrusions are characteristic for the veneering of the Ti6Al4V substructure with SLM **(Fig. 12a)**. In defects, the structure is very irregular, with visible flaky abrasions and furrows **(Fig. 10b, Fig. 11b, Fig. 12b)**. There are jagged and irregular edges of the defects in the TiCP and Ti6Al4V substructures from milling **(Fig. 10c, Fig. 11c)**. The most regular shape of the defect edge occurred at the substructure of Ti6Al4V with SLM **(Fig. 12c)**.

Fig. 10. **SEM images of the surface veneering Vita Titankeramik ceramics on the TiCP milled substructure: a) surface layer developed at the clinical level, b) surface layer in the defect after the wear test, c) border zone between the defect and the area before the wear test**

Rys. 10. Obrazy SEM powierzchni licowanej ceramiką Vita Titankeramik na podbudowie TiCP frezowanej: a) warstwa wierzchnia opracowana na poziomie klinicznym, b) warstwa wierzchnia w skazie po badaniu zużyciowym, c) strefa granicy między skazą a obszarem przed badaniem zużyciowym
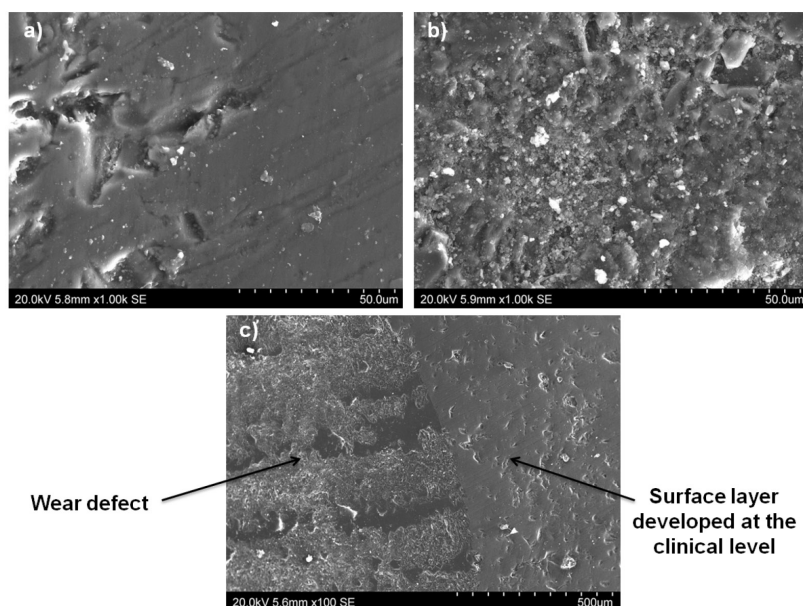

Fig. 11. **SEM images of the surface veneered with Vita Titankeramik ceramics on the Ti6Al4V milled substructure: a) surface layer developed at the clinical level, b) surface layer in the defect after the wear test, c) border zone between the defect and the area before the wear test**

Rys. 11. Obrazy SEM powierzchni licowanej ceramiką Vita Titankeramik na podbudowie Ti6Al4V frezowanej: a) warstwa wierzchnia opracowana na poziomie klinicznym, b) warstwa wierzchnia w skazie po badaniu zużyciowym, c) strefa granicy między skazą a obszarem przed badaniem zużyciowym
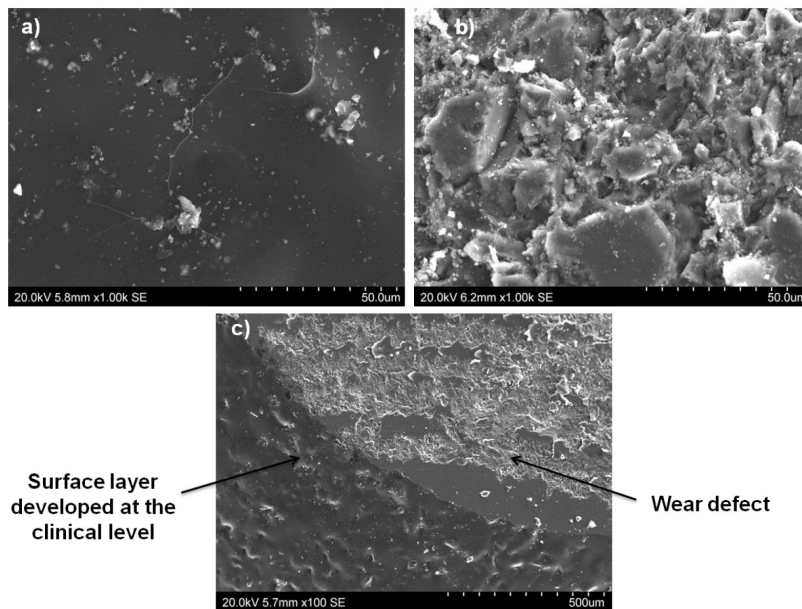
Fig. 12. SEM images of the surface veneered with Vita Titankeramik ceramics on Ti6Al4V incremental sintering substructure: a) surface layer developed at the clinical level, b) surface layer in defects after the wear test, c) border zone between the defects and the area before the wear test

Rys. 12. Obrazy SEM powierzchni licowanej ceramiką Vita Titankeramik na podbudowie Ti6Al4V z przyrostowego spiekania: a) warstwa wierzchnia opracowana na poziomie klinicznym, b) warstwa wierzchnia w skazie po badaniu zużyciowym, c) strefa granicy między skazą a obszarem przed badaniem zużyciowym

SEM images of the surface veneered with the IPS e.max Ceram ceramics on glass and the ceramic $LiSi_2$ substructure from milling are characterized by numerous pores and rounded protrusions **(Fig. 13a)**. The surface is smooth throughout the image. The edge of the defect is regular, i.e. in the wiping zone there is a regular structure with a few defects and products of wear **(Fig. 13c)**. Large polished areas, numerous tears, and bumps are visible in the defects **(Fig. 13b)**.

The SEM image of the surface veneered with Elephant Sakura ceramics on the ZrO_2 substructure is characterized by a uniform structure with very few pores and cavities **(Fig. 14a)**. The surface in defects is very regular; there is no exfoliation and the boundaries of the vitreous phase surrounding the crystalline phase are barely visible **(Fig. 14b)**. The edge of the defect is very regular **(Fig. 14c)**. A few products of wear are visible in the defect. The surface is very smooth before wear and in the case of wear defects.

DISCUSSION OF TEST RESULTS

In layered biomaterials veneering prosthetic structures, the processes of surface layer destruction are different from those destroying enamel **[L. 4–6, 12, 15–18]**. Based on enamel structure studies, it can be assumed

that the strong mineralization of enamel tissue and the distribution of prisms under the surface layer lead to tribological processes having a specific course **(Fig. 15)**. A stochastically oriented system of enamel prisms, their strength parameters, and their physical and chemical compatibility with saliva influence the low friction coefficient in comparison to ceramic biomaterials veneering prosthetic structures. The course and very similar values of friction coefficients in the testing of veneering layers do not translate into different wear resistance results evaluated on the basis of average diameters of wear defects.

Analysis of the results of the wear of veneering on metal substructures made of CoCrMo and titanium indicates that the average value of wear depends on the hardness and Young's module of the structure on which the veneering was carried out **[L. 9]**. The lower the values of the substructure and the lower the Young's module, the smaller are the diameters of the wear defects, i.e. the material was more resistant to wear. The wear resistance of the veneering layer may be affected by the strength parameters of the substructure, but primarily by the microgeometry, structure, the adhesion of the sprayed ceramic layers, and compatibility with saliva **[L. 8, 19–24]**.

Tests of enamel wear resistance performed to compare its tribological parameters and the wear
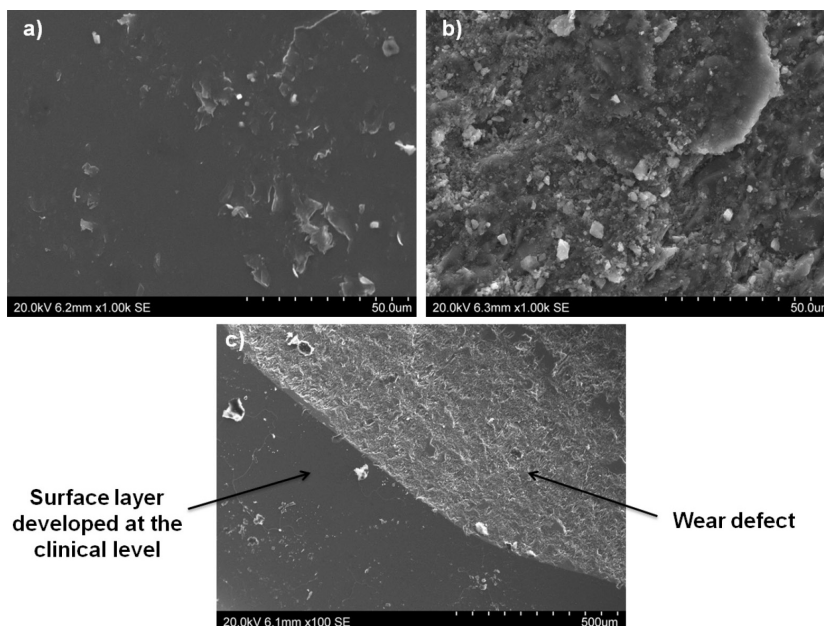
Fig. 13. SEM images of the surface veneered with IPS e.max Ceram ceramics on the milled LiSi$_2$ substructure: a) surface layer developed at the clinical level, b) surface layer in the defect after the wear test, c) border zone between the defect and the area before the wear test

Rys. 13. Obrazy SEM powierzchni licowanej ceramiką IPS e.max Ceram na podbudowie LiSi$_2$ frezowanej: a) warstwa wierzchnia opracowana na poziomie klinicznym, b) warstwa wierzchnia w skazie po badaniu zużyciowym, c) strefa granicy między skazą a obszarem przed badaniem zużyciowym
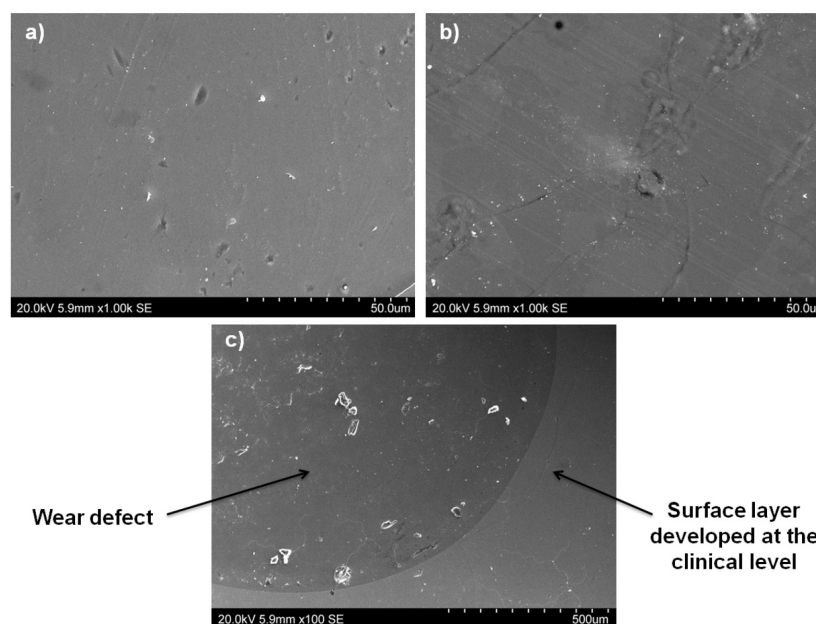

Fig. 14. SEM images of the surface veneered with Elephant Sakura ceramics on the ZrO$_2$ milled and sintered substructure: a) surface layer developed at the clinical level, b) surface layer in the defect after the wear test, c) border zone between the defect and the area before the wear test

Rys. 14. Obrazy SEM powierzchni licowanej ceramiką Elephant Sakura na podbudowie ZrO$_2$ frezowanej i spiekanej: a) warstwa wierzchnia opracowana na poziomie klinicznym, b) warstwa wierzchnia w skazie po badaniu zużyciowym, c) strefa granicy między skazą a obszarem przed badaniem zużyciowym
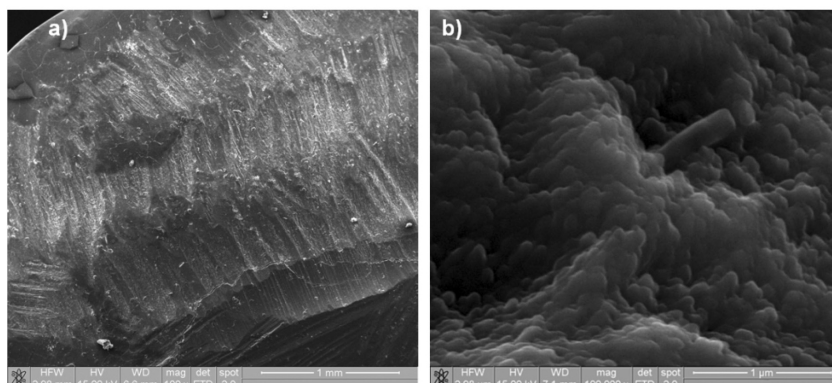
Fig. 15. SEM images of enamel prisms [L. 15]
Rys. 15. Obrazy SEM pryzmatów szkliwnych **[L. 15]**

resistance of nanocomposites for direct restoration showed that the average diameter of defects on enamel and dentin discs was at the level of 3.14 mm **[L. 15]**.

The SEM analyses carried out allowed us to assess the veneering of the substructure after the firing of opaque, dentin, and enamel layers as well as after the tribological test in the wear defect. Based on the presented edges of wear defects, it can be concluded that the more regular the line of the circle, without breaks and visible wear products, the more stable is the process and the wear is of an adaptive nature **[L. 25–28]**.

CONCLUSIONS

The applied test method, combining biomechanical analysis of wear resistance with microstructure analysis, allows the tribological properties of ceramic layers veneering prosthetic supporting substructures with digital technologies to be assessed.

All the biomaterials tested are suitable for the veneering of support structures used in clinical conditions, i.e. they ensure a slightly higher level of wear resistance than those found in natural normal chewing organ tissues.

In the studied veneering ceramics, in terms of wear resistance and uniform fine-grained microstructure, the Elephant Sakura system used for the ZrO_2 substructure obtained from the milling technology in CAD/CAM and sintering is worth mentioning.

ACKNOWLEDGEMENT

REFERENCES

1. Gołębiowski M., Wolowiec E., Klimek L.: Airborne-particle abrasion parameters on the quality of titanium-ceramic bonds. The Journal of Prosthetic Dentistry, 113, 5(2015), pp. 453–459.
2. Nguyen H.H., Wan S., Tieu K.A., Pham S.T., Zhu H.: Tribological behaviour of enamel coatings. Wear, 426(2019), pp. 319–329.
3. Guo J., Tian B., Wei R., Wang W., Zhang H., Wu X., He L., Zhang S.: Investigation of the time-dependent wear behavior of veneering ceramic in porcelain fused to metal crowns during chewing simulations. Journal of the Mechanical Behavior of Biomedical Materials, 40(2014), pp. 23–32.
4. Naumova E., Schneider S., Arnold W., Piwowarczyk A.: Wear behavior of ceramic CAD/CAM crowns and natural antagonists. Materials, 10, 3(2017), p. 244.
5. Wang L., Liu Y., Si W., Feng H., Tao Y., Ma Z.: Friction and wear behaviors of dental ceramics against natural tooth enamel. Journal of the European Ceramic Society, 32, 11(2012), pp. 2599–2606.
6. Mitov G., Heintze S.D., Walz S., Woll K., Muecklich F., Pospiech P.: Wear behavior of dental Y-TZP ceramic against natural enamel after different finishing procedures. Dental Materials, 28, 8(2012), pp. 909–918.
7. Ryniewicz A.M., Ryniewicz W., Bojko Ł., Pałka P.: Tribological tests and impact tests of acrylic polymers for dental prosthetics. Tribologia, 4(2018), pp. 89–95.
8. Sinthuprasirt P., van Noort R., Moorehead R., Pollington S.: Evaluation of a novel multiple phase veneering ceramic. Dental Materials, 31, 4(2015), pp. 443–452.

9.   Bojko Ł., Ryniewicz W., Ryniewicz A.M., Kot M., Pałka P.: The influence of additive technology on the quality of the surface layer and the strength structure of prosthetic crowns. Tribologia. 4(2018), pp. 13–22.

10. Ryniewicz W., Ryniewicz A.M., Bojko Ł.: The effect of a prosthetic crown's design on the accuracy of mapping an abutment teeth's shape. Measurement, 91(2016), pp. 620–627.

11. Grohmann P., Bindl A., Hämmerle C., Mehl A., Sailer I.: Three-unit posterior zirconia-ceramic fixed dental prostheses (FDPs) veneered with layered and milled (CAD-on) veneering ceramics: 1-year follow-up of a randomized controlled clinical trial. Quintessence International, 46, 10(2015), pp. 871–880.

12. Song W., Wang X., Jiao J.: Comparative study of four crown materials and enamel on the wearing ability in vitro. Journal of Modern Stomatology, 4(2015), 12.

13. Biben A., Ozhohan Z.: Clinical Effectiveness of Using Aesthetic Fixed Prosthetic Appliances with Combined Occlusal Surface. Galician Medical Journal, 24, 2(2017), E201725.

14. Bianchi E.C., da Silva E.J., Monici R.D., de Freitas C.A., Bianchi A.R.R.: Development of new standard procedures for the evaluation of dental composite abrasive wear. Wear, 253, 5(2002), pp. 533–540.

15. Ryniewicz W., Herman M., Ryniewicz A.M., Bojko Ł., Pałka P., Ryniewicz A., Madej T.: Tribological tests of the nanomaterials used to reconstruct molars and premolars with the application of the direct method. Tribologia, 3(2017), pp. 155–164.

16. Herman M., Ryniewicz A.M., Ryniewicz W.: The analysis of determining factors of enamel resistance to wear. Pt. 1, Identification of biological and mechanical enamel structure and its shape in dental crowns. Engineering of Biomaterials, 13, 95(2010), pp. 10–17.

17. Ryniewicz W., Herman M., Ryniewicz A.M.: The analysis of enamel resistance to wear determining factors. Pt. 2, Study of superficial layer and microhardness in tooth enamel. Engineering of Biomaterials, 14, 102(2011), pp. 23–27.

18. Ryniewicz W., Herman M., Ryniewicz A.M., Bojko Ł., Pałka P.: Badania tribologiczne nanokompozytów do odbudowy bezpośredniej zębów. Tribologia, 4(2018), pp. 97–105.

19. Mainjot A.K., Najjar A., Jakubowicz-Kohen B.D., Sadoun M.J.: Influence of thermal expansion mismatch on residual stress profile in veneering ceramic layered on zirconia: Measurement by hole-drilling. Dental Materials, 31, 9(2015), pp. 1142–1149.

20. Luo H., Tang X., Dong Z., Tang H., Nakamura T., Yatani H.: The influences of accelerated aging on mechanical properties of veneering ceramics used for zirconia restorations. Dental Materials Journal, 35, 2(2016), pp. 187–193.

21. Antanasova M., Kocjan A., Kovač J., Žužek B., Jevnikar P.: Influence of thermo-mechanical cycling on porcelain bonding to cobalt–chromium and titanium dental alloys fabricated by casting, milling, and selective laser melting. Journal of Prosthodontic Research, 62, 2(2018), pp. 184–194.

22. Souza J.C., Henriques M., Teughels W., Ponthiaux P., Celis J.P., Rocha L.A.: Wear and corrosion interactions on titanium in oral environment: literature review. Journal of Bio-and Tribo-Corrosion, 1, 2(2015), 13.

23. Buciumeanu M., Bagheri A., Shamsaei N., Thompson S.M., Silva F.S., Henriques B.: Tribocorrosion behavior of additive manufactured Ti-6Al-4V biomedical alloy. Tribology International, 119(2018), pp. 381–388.

24. Souza J.C., Tajiri H.A., Morsch C.S., Buciumeanu M., Mathew M.T., Silva F.S., Henriques B.: Tribocorrosion behavior of Ti6Al4V coated with a bio-absorbable polymer for biomedical applications. Journal of Bio-and Tribo-Corrosion, 1, 4(2015), 27.

25. Santos R.L.P., Buciumeanu M., Silva F.S., Souza J.C.M., Nascimento R.M., Motta F.V., Carvalho O., Henriques B.: Tribological behaviour of glass-ceramics reinforced by Yttria Stabilized Zirconia. Tribology International, 102(2016), pp. 361–370.

26. Figueiredo-Pina C.G., Patas N., Canhoto J., Cláudio R., Olhero S.M., Serro A.P., Ferro A.C., Guedes M.: Tribological behaviour of unveneered and veneered lithium disilicate dental material. Journal of the Mechanical Behavior of Biomedical Materials, 53 (2016), pp. 226–238.

27. Figueiredo-Pina C.G., Monteiro A., Guedes M., Mauricio A., Serro A.P., Ramalho A., Santos C.: Effect of feldspar porcelain coating upon the wear behavior of zirconia dental crowns. Wear, 297, 1–2 (2013), pp. 872–877.

28. Preis V., Behr M., Kolbeck C., Hahnel S., Handel G., Rosentritt M.: Wear performance of substructure ceramics and veneering porcelains. Dental Materials, 27, 8(2011), pp. 796–804.